37th EPS Conference on Plasma Physics P5.152

A multi-tile-electrode plasma source for large-area negative-ion production for neutral beam heating of ITER

Thomas Gilmore[1,2], Thomas Rudden[1,2], Kevin Ryan[2], David O'Farrell[1,2],

Cezar Gaman[2] and A.R. Ellingboe[1,2]

[1]Phive Plasma Technologies, DCU/Invent, Glasnevin, Ireland

[2]Plasma Research lab, School of Physical Sciences and NCPST, Dublin City University, Ireland

Abstract

We evaluate a multi-tile-electrode plasma source for application to the production of negative hydrogen ions for use in neutral-beam heating of ITER. We present a scaled plasma-source design (300mm x 400mm) with a continuously variable magnetic field parallel to the plasma-grid plane. Plasma density above the plasma-grid-plane is enhanced by the magnetic filter-field. Plasma density measurements show that the filter field affects the plasma transport by modifications to the power coupling from the electrode tiles as the cyclotron frequency approaches the rf-drive frequency. This design allows for a lower dipole-field strength adjacent to the source than the reference ITER design, which reduces interference with the ion accelerator.[1]

Pastis Applied as a Neutral Injection Beam Plasma Source

To aid the heating process of confined plasmas in toroidal fusion chambers, high-powered beams of neutral atoms are injected into the system, depositing their energy through collisions. The plasma source for the ITER neutral beam reference design employs eight 2MHz inductive plasma sources feeding into a diffusion region and filter field to reduce the electron temperature and facilitate extraction grid biasing to reduce ion bombardment energy. To produce H- ions, H+ ions collide with the caesiated extraction grid which has a very low work function. If the H+ ions have low enough energy (< 2eV), there is a finite probability that it will leave the surface with two electrons, forming H-.[2] The difficulty is creating the very high flux of H+ ions for the beam while maintaining the necessary low energies of those ions. The large, unbounded nature of the reference design combined with the filter field requirement results in a large total magnetic flux, and the dipole field has negative effects on the accelerator and transport to the neutralizer.

The Pastis system is 300mm x 400mm rectangular plasma source, similar in area to the Kamaboko-III and BATMAN systems, but only 7cm in height between the rf antennae and the location of the (hypothetical) extraction grid. The plasma source resembles a capacitive diode, but where the upper electrode is segmented into a 3 x 4 tile array. Two representative tiles are shown in Figure 1. These two, adjacent half-tiles can be considered as a 'unit-cell' of the plasma source. RF power is delivered differentially between adjacent tiles. The rf voltage on tiles drives displacement current in the sheath and gives electrostatic (ES) coupling. The skin-depth ($\lambda=c/\omega_{pe}$) is substantially smaller than the chamber height. The rf currents in the tiles (as shown by the current vectors in figure 1) couple electromagnetically (EM) to the plasma, driving image currents parallel to the sheath-edge. The current is in-phase across the tile-gap, and the rf-dipole-field formed by the tile-edges further boost the EM induced field at the gap. This source topology has the advantage that it is extendable in area for scaling to application on ITER, has 1-dimensional plasma transport from the source to the extraction grid, 1-D transport of Caesium, and the filter field can be formed as a solenoid with substantially lower field amplitude in the accelerator and transport to the neutralizer.

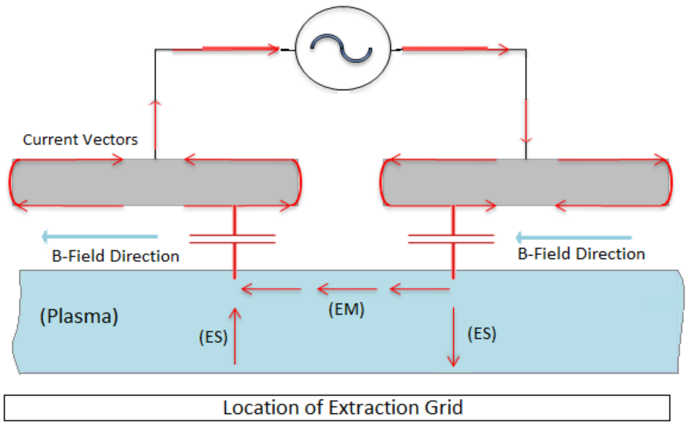

Figure 1: Pastis source operation

Previous work in an unmagnetized version of the source operated at 400 MHz demonstrated efficiencies, approaching 88 eV / e-ion pair, suggesting the multi-tile-electrode topology can achieve very high plasma efficiency. [3]

In the present work, Pastis is operated with rf excitation at 162 MHz, at powers ranging from 300W to 1.5kW, Argon gas at a pressure of 10 mTorr and with magnetic field parallel to the plasma-grid plane continuously variable between 20 and 70 Gauss. In this field range, magnetized electrons have cyclotron frequencies ($f_{CE} = eB/2\pi m$) between 56 MHz and 196 MHz. At 60 Gauss and at electron energies of 2eV (thermal) to 11.7eV (threshold for 2-step ionization in argon), the Larmor radius of the electrons ranges from 0.5 – 1.4mm. We will measure the density to be on the order of 10^{10} cm^{-3}, resulting in Debye length of 10 -

100µm and skin depth on the order of 1cm. The electron-neutral mean-free-path for energetic electrons is approximately 20cm, so the electrons are weakly to moderately magnetized.[4]

Ion saturation current is measured using a single-sided planar Langmuir probe biased to -36 V. The 4.7mm diameter probe-tip is positioned 5cm from the centre of a tile-face. Plasma density can be approximated from $n = (I/eA) * (kT_e/M_i)^{1/2}$, where I is the measured current and A is the probe area. Assuming the electron temperature is uniformly 2eV, $1mA/cm^2$ equates to approximately $3x10^{10}cm^{-3}$.

Experimental Data and Results

Figure 2 presents the measured ion flux versus magnetic field at 300 watts rf power. Two peaks are seen, occurring at magnetic fields where f_{CE} = ½ f_{RF} (29G) and f_{CE} = f_{RF} (58G). Noting that the ES fields are perpendicular to the externally imposed magnetic field, this is interpreted as an interaction between the ES fields with the magnetized electrons in a cyclotron heating mechanism. The Larmor radius is greater than the Debye length, so the gyrating electrons escape the oscillating rf field for most of their orbit. At f_{CE} = ½ f_{RF} and f_{CE} = f_{RF}, some of the plasma's electrons will re-enter the sheath in phase with expanding sheath edge, accentuating ES power transfer through cyclotron heating for multiple rf power cycles. The plasma density between the peaks is higher than at 20 Gauss, and this is interpreted as magnetization of the electrons reducing the cross-field diffusion and the resultant loss-rate at the extraction plane. The drop in density above 60 gauss may be due to the probe position being close to the extraction plane, and for strongly magnetized electrons the preferential loss mechanism is transport along the magnetic field, rather than cross-field to the probe.

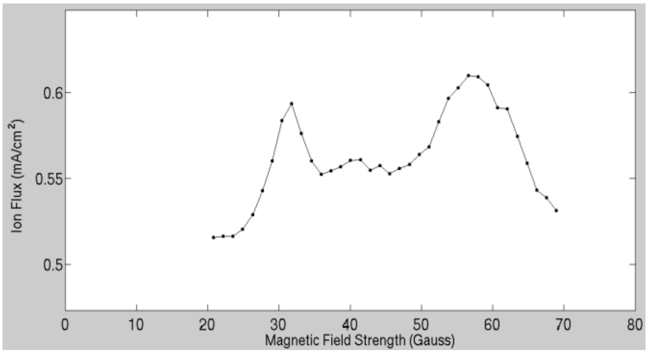

Figure 2: Plot of ion flux against magnetic field at a pressure of 10 milliTorr at a power of 300 watts

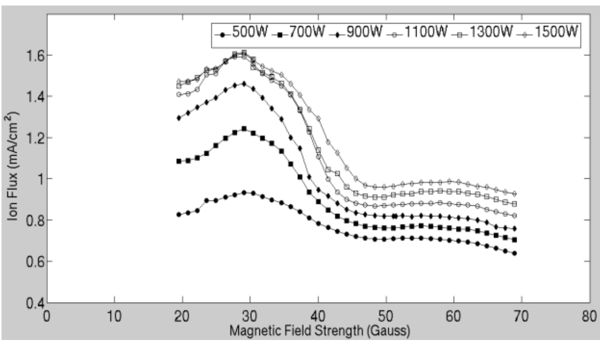

Figure 3: Ion flux against magnetic field for a range of rf

Figure 3 shows ion flux versus magnetic field at select powers. Ion flux increases with power. The peak at f_{CE}=½ f_{RF}

continues to be evident, however, the peak at $f_{CE} = f_{RF}$ is not clearly pronounced. Figure 4 shows the ion flux at the two resonant conditions (29 and 58 Gauss) versus power.

The results are consistent with the following interpretation. The density is dependent on particle balance based on the ionization source-term and losses. The losses change with magnetic field, as the characteristic length of the system changes from half-height of 3.5cm (no magnetization) to half-length of 22cm (fully magnetized.) The source term is dependent on both ES and EM coupling. The saturation in ion flux with power at 29 Gauss is consistent with a decreasing ES power coupling which scales with the square-root of power. The EM coupling, which dominates at high power/density scales linearly with power and is independent of magnetic field, as the EM electric field is parallel to the externally imposed magnetic field. The cyclotron power coupling at the higher field (58G) is suppressed before it is suppressed at the lower magnetic field (29G). This is understood based on the ES power deposition dependence on magnetic field. The ES power deposition, including the enhanced component due to cyclotron effects, is closer to the tiles at high magnetic field. This results in increased ionization close to the tiles which, in turn, enhances the EM power coupling, which further suppresses the ES power transfer.

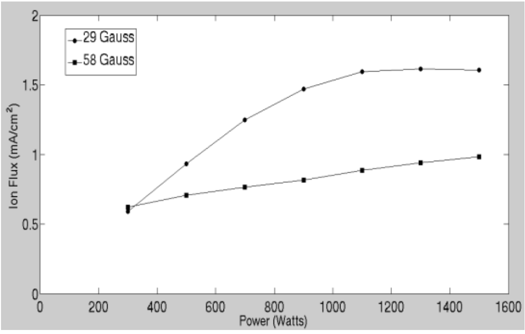

Figure 4: Ion flux for selected rf-powers at the resonant peaks at 29G and 58G

The advantages based on the 1-D plasma and caesium transport and the reduction in magnetic field dipole suggest that this is worthy of consideration as a back-up to the ITER reference design.

References

[1] R.Hemsworth et al., *"Status of the ITER heating neutral beam system".* IOP publishing and International Atomic Energy Agency. Published at stacks.iop.org/NF/49/045006, March 2009.

[2] K.Shinto et al., "*Correlation between Negative Ion Production and Work Function of Plasma Grid Surface in a Caesium-Introduced Volume-Production-Type Negative Hydrogen Ion Source"*, Jpn. J. Appl. Phys. Vol. 35 (1996) pp. 1894-1900.

[3] A.R Ellingboe et al., "*A 2-D scalable, VHF/UHF compatible, capacity coupled plasma source for large-area applications*".

[4] H.B. Wahlin, "*The Motion of Electrons in Argon*", Physical Review Vol. 37.